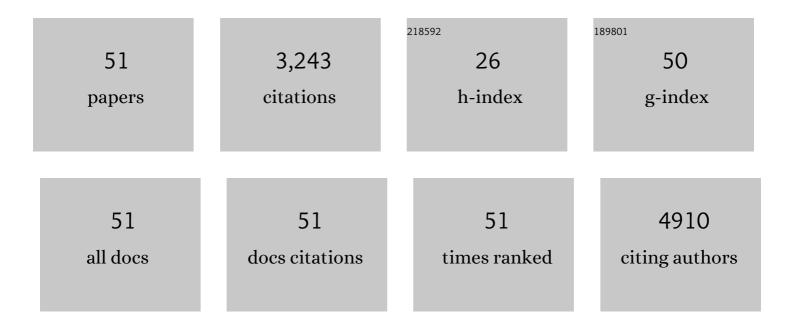


## List of Publications by Year in descending order

Source: https://exaly.com/author-pdf/4820708/publications.pdf Version: 2024-02-01



OIN LI

#	Article	IF	CITATIONS
1	Self-powered textile for wearable electronics by hybridizing fiber-shaped nanogenerators, solar cells, and supercapacitors. Science Advances, 2016, 2, e1600097.	4.7	705
2	Blow-driven triboelectric nanogenerator as an active alcohol breath analyzer. Nano Energy, 2015, 16, 38-46.	8.2	255
3	Harvesting Broad Frequency Band Blue Energy by a Triboelectric–Electromagnetic Hybrid Nanogenerator. ACS Nano, 2016, 10, 6526-6534.	7.3	244
4	A Waterâ€Proof Triboelectric–Electromagnetic Hybrid Generator for Energy Harvesting in Harsh Environments. Advanced Energy Materials, 2016, 6, 1501593.	10.2	243
5	Preparation of ZnFe <sub>2</sub> O <sub>4</sub> nanostructures and highly efficient visible-light-driven hydrogen generation with the assistance of nanoheterostructures. Journal of Materials Chemistry A, 2015, 3, 8353-8360.	5.2	135
6	Efficient Energy Funneling in Quasiâ€2D Perovskites: From Light Emission to Lasing. Advanced Materials, 2020, 32, e1906571.	11.1	134
7	Effective Formation of Oxygen Vacancies in Black TiO <sub>2</sub> Nanostructures with Efficient Solar-Driven Water Splitting. ACS Sustainable Chemistry and Engineering, 2017, 5, 8982-8987.	3.2	131
8	Highly transparent and conducting fluorine-doped ZnO thin films prepared by pulsed laser deposition. Solar Energy Materials and Solar Cells, 2011, 95, 894-898.	3.0	116
9	Controllable synthesis of Co3O4 crossed nanosheet arrays toward an acetone gas sensor. Sensors and Actuators B: Chemical, 2017, 238, 1052-1059.	4.0	98
10	Gas sensors based on ultrathin porous Co <sub>3</sub> O <sub>4</sub> nanosheets to detect acetone at low temperature. RSC Advances, 2015, 5, 59976-59982.	1.7	96
11	Extended Light Harvesting with Dual Cu <sub>2</sub> Oâ€Based Photocathodes for High Efficiency Water Splitting. Advanced Energy Materials, 2018, 8, 1702323.	10.2	93
12	A facile fluorine-mediated hydrothermal route to controlled synthesis of rhombus-shaped Co3O4 nanorod arrays and their application in gas sensing. Journal of Materials Chemistry A, 2013, 1, 7511.	5.2	91
13	Synthesis of TiO <sub>2</sub> decorated Co <sub>3</sub> O <sub>4</sub> acicular nanowire arrays and their application as an ethanol sensor. Journal of Materials Chemistry A, 2015, 3, 2794-2801.	5.2	73
14	Hollowsphere Nanoheterojunction of g-C <sub>3</sub> N <sub>4</sub> @TiO <sub>2</sub> with High Visible Light Photocatalytic Property. Langmuir, 2019, 35, 779-786.	1.6	70
15	A two-step synthesis of nanosheet-covered fibers based on α-Fe2O3/NiO composites towards enhanced acetone sensing. Scientific Reports, 2018, 8, 1705.	1.6	53
16	The crystalline/amorphous contact in Cu <sub>2</sub> O/Ta <sub>2</sub> O <sub>5</sub> heterostructures: increasing its sunlight-driven overall water splitting efficiency. Journal of Materials Chemistry A, 2017, 5, 2732-2738.	5.2	41
17	Fabrication of Fe <sub>2</sub> TiO <sub>5</sub> /TiO <sub>2</sub> nanoheterostructures with enhanced visible-light photocatalytic activity. RSC Advances, 2016, 6, 45343-45348.	1.7	38
18	Robust Aboveâ€Roomâ€Temperature Ferromagnetism in Few‣ayer Antimonene Triggered by Nonmagnetic Adatoms. Advanced Functional Materials, 2019, 29, 1808746.	7.8	38

Qin Li

#	Article	IF	CITATIONS
19	A two-step synthesis of microsphere-decorated fibers based on NiO/ZnSnO3 composites towards superior ethanol sensitivity performance. Journal of Alloys and Compounds, 2019, 777, 73-83.	2.8	38
20	Understanding the Role of Ion Migration in the Operation of Perovskite Light-Emitting Diodes by Transient Measurements. ACS Applied Materials & Interfaces, 2020, 12, 48845-48853.	4.0	37
21	A new type of hybrid nanostructure: complete photo-generated carrier separation and ultrahigh photocatalytic activity. Journal of Materials Chemistry A, 2014, 2, 14245-14250.	5.2	36
22	Directional Polarized Light Emission from Thinâ€Film Lightâ€Emitting Diodes. Advanced Materials, 2021, 33, e2006801.	11.1	35
23	A new type of p-type NiO/n-type ZnO nano-heterojunctions with enhanced photocatalytic activity. RSC Advances, 2014, 4, 34649.	1.7	30
24	Highly transparent conductive F-doped ZnO films in wide range of visible and near infrared wavelength deposited on polycarbonate substrates. Journal of Alloys and Compounds, 2014, 614, 71-74.	2.8	30
25	Acceptor defect-participating magnetic exchange in ZnO : Cu nanocrystalline film: defect structure evolution, Cu–N synergetic role and magnetic control. Journal of Materials Chemistry C, 2015, 3, 1330-1346.	2.7	28
26	Interfacial study of Cu <sub>2</sub> O/Ga <sub>2</sub> O <sub>3</sub> /AZO/TiO <sub>2</sub> photocathode for water splitting fabricated by pulsed laser deposition. Catalysis Science and Technology, 2017, 7, 1602-1610.	2.1	26
27	Highly conductive thin films of nonmetal F and B co-doped ZnO on flexible substrates: Experiment and first-principles calculations. Journal of Alloys and Compounds, 2017, 697, 156-160.	2.8	25
28	ZnO/TiO2 core–shell nanowire arrays for enhanced dye-sensitized solar cell efficiency. Applied Physics A: Materials Science and Processing, 2013, 113, 67-73.	1.1	24
29	P-Type Cobalt Phosphide Composites (CoP–Co <sub>2</sub> P) Decorated on Titanium Oxide for Enhanced Noble-Metal-Free Photocatalytic H <sub>2</sub> Evolution Activity. Langmuir, 2021, 37, 3321-3330.	1.6	24
30	Humidity sensor based on mesoporous Al-doped NiO ultralong nanowires with enhanced ethanol sensing performance. Journal of Materials Science: Materials in Electronics, 2019, 30, 7121-7134.	1.1	23
31	Synthesis of Co3O4/Ta2O5 heterostructure hollow nanospheres for enhanced room temperature ethanol gas sensor. Journal of Alloys and Compounds, 2017, 727, 436-443.	2.8	21
32	Coaxial electrospinning Fe2O3@Co3O4 double-shelled nanotubes for enhanced ethanol sensing performance in a wide humidity range. Journal of Alloys and Compounds, 2022, 891, 161868.	2.8	21
33	Surface modification and stoichiometry control of Cu2O/SnO2 heterojunction solar cell by an ultrathin MgO tunneling layer. Journal of Alloys and Compounds, 2019, 779, 387-393.	2.8	20
34	Interfacial effect on Mn-doped TiO <sub>2</sub> nanoparticles: from paramagnetism to ferromagnetism. RSC Advances, 2016, 6, 57403-57408.	1.7	18
35	Ultrahigh efficient water oxidation under visible light: Using Fe dopants to integrate nanostructure and cocatalyst in LaTiO2N system. Nano Energy, 2016, 19, 437-445.	8.2	17
36	Ultrasensitive Sensors Based on PdO@SrFe <sub>2</sub> O <sub>4</sub> Nanosphere-Modified Fibers for Real-Time Monitoring of Ethanol Gas. ACS Applied Electronic Materials, 2021, 3, 1732-1746.	2.0	17

Qin Li

#	Article	IF	CITATIONS
37	Twoâ€Step Plasma Treatment Designed for Highâ€Performance Flexible Amorphous ZnAlSnO Thinâ€Film Transistors Replacing Thermal Annealing. Advanced Electronic Materials, 2020, 6, 2000233.	2.6	16
38	Origin of highly stable conductivity of H plasma exposed ZnO films. Physical Chemistry Chemical Physics, 2013, 15, 17763.	1.3	15
39	Carbon Sphere Template Derived Hollow Nanostructure for Photocatalysis and Gas Sensing. Nanomaterials, 2020, 10, 378.	1.9	13
40	Enhanced Surface Passivation of Lead Sulfide Quantum Dots for Short-Wavelength Photodetectors. Chemistry of Materials, 2022, 34, 5433-5442.	3.2	13
41	Enhanced photoelectrochemical water-splitting performance of SrNbO2N photoanodes using flux-assisted synthesis method and surface defect management. Sustainable Energy and Fuels, 2020, 4, 1674-1680.	2.5	10
42	Low-Temperature Detection of Sulfur-Hexafluoride Decomposition Products Using Octahedral Co <sub>3</sub> O <sub>4</sub> -Modified NiSnO <sub>3</sub> Nanofibers. ACS Applied Materials & Interfaces, 2022, 14, 9292-9306.	4.0	10
43	A solution processed Sb <sub>2</sub> S <sub>3</sub> -based photocathode with enhanced photocatalytic performance <i>via</i> constructing an ultrathin TiO <sub>2</sub> overlayer and noble metal modification. Sustainable Energy and Fuels, 2021, 5, 855-861.	2.5	8
44	One-step controllable synthesis of amino-modification siloxene for enhanced solar water-splitting. Journal of Colloid and Interface Science, 2020, 579, 205-211.	5.0	7
45	Interaction of H and F atoms—Origin of the high conductive stability of hydrogen-incorporated F-doped ZnO thin films. Thin Solid Films, 2015, 589, 85-89.	0.8	6
46	Room temperature monitoring of SF <sub>6</sub> decomposition byproduct SO <sub>2</sub> F <sub>2</sub> based on TiO <sub>2</sub> /NiSO <sub>4</sub> composite nanofibers. Nanotechnology, 2021, 32, 305705.	1.3	6
47	Light extraction in tandem organic light emitting diodes. Applied Physics Letters, 2021, 119, .	1.5	6
48	Electric-field driven insulator-metal transition and tunable magnetoresistance in ZnO thin film. Applied Physics Letters, 2018, 112, .	1.5	5
49	Electricâ€Field Control of Dirac Twoâ€Dimensional Electron Gas in PbTe/CdTe Heterostructures. Physica Status Solidi - Rapid Research Letters, 2019, 13, 1800551.	1.2	3
50	2D Ferromagnetism: Robust Aboveâ€Roomâ€Temperature Ferromagnetism in Fewâ€Layer Antimonene Triggered by Nonmagnetic Adatoms (Adv. Funct. Mater. 15/2019). Advanced Functional Materials, 2019, 29, 1970099.	7.8	1
51	27â€4: Organic Lightâ€Emitting Diodes with Directional Polarized Light Emission. Digest of Technical Papers SID International Symposium, 2021, 52, 345-348.	0.1	0